

before, most recently in those of the respective tetramethylammonium salts.<sup>15</sup>

Crystal structure determinations of the remaining complexes of the system, with 5 to 8 mol of hydrogen fluoride per mol of pyridine, will most probably reveal these as pyridinium poly(hydrogen fluorides), too. Anions  $H_4F_5^-$  and, in one instance each,  $H_5F_6^-$  and  $H_7F_8^-$  are already established species in the solid state.<sup>6,15</sup>

(15) Mootz, D.; Boenigk, D. Z. *Anorg. Allg. Chem.* 1987, 544, 159-166.

**Acknowledgment.** This work was supported by the Minister für Wissenschaft und Forschung des Landes Nordrhein-Westfalen and by the Fonds der Chemischen Industrie.

**Registry No.**  $C_5H_5N$ , 110-86-1; HF, 7664-39-3;  $C_5H_5N \cdot HF$ , 32001-55-1;  $C_5H_5N \cdot 2HF$ , 87979-78-0;  $C_5H_5N \cdot 3HF$ , 79162-49-5;  $C_5H_5N \cdot 4HF$ , 85351-48-0.

**Supplementary Material Available:** Listing of anisotropic thermal parameters for the non-hydrogen atoms (2 pages); structure factor tables (8 pages). Ordering information is given on any current masthead page.

## Kinetics, Mechanisms, and Catalysis of Oxygen Atom Transfer Reactions of *S*-Oxide and Pyridine *N*-Oxide Substrates with Molybdenum(IV,VI) Complexes: Relevance to Molybdoenzymes

John P. Caradonna,<sup>1a</sup> P. Rabindra Reddy,<sup>1b</sup> and R. H. Holm\*

Contribution from the Department of Chemistry, Harvard University, Cambridge, Massachusetts 02138. Received August 10, 1987

**Abstract:** The kinetics and mechanism of the oxygen atom transfer reactions  $MoO_2(L-NS_2) + (R_F)_3P \rightarrow MoO(L-NS_2)(DMF) + (R_F)_3PO$  (1) and  $MoO(L-NS_2)(DMF) + XO \rightarrow MoO_2(L-NS_2) + X$ , with  $X = (R_F)_2SO$  (2) and 3-fluoropyridine *N*-oxide (3), have been investigated in DMF solutions ( $L-NS_2 = 2,6$ -bis(2,2-diphenyl-2-mercaptoethyl)pyridine(2-),  $R_F = p-C_6H_4F$ ). The following rate constants (297.5 K) and activation parameters were obtained: reaction 1,  $k_2 = 9.7$  (4)  $\times 10^{-3} M^{-1} s^{-1}$ ,  $\Delta H^\ddagger = 11.7$  (6) kcal/mol,  $\Delta S^\ddagger = -28.4$  (1.6) eu; reaction 2,  $k_1 = 14.0$  (7)  $\times 10^{-4} s^{-1}$ ,  $\Delta H^\ddagger = 22.1$  (1.3) kcal/mol,  $\Delta S^\ddagger = 2.6$  (1.6) eu; reaction 3,  $k_1 = 16.0$  (8)  $\times 10^{-4} s^{-1}$ ,  $\Delta H^\ddagger = 23.4$  (1.4) kcal/mol,  $\Delta S^\ddagger = 7.2$  (2.0) eu. Reactions 2 and 3 exhibit saturation kinetics, under which the rate-determining step is intramolecular atom transfer. Mechanisms and transition states are proposed. The activation parameters are the first measured for oxo transfer from substrate; the small activation entropies suggest a transition state structurally similar to the complex  $MoO(L-NS_2)(XO)$  formed in a labile equilibrium prior to oxo transfer to Mo. Coupling of reaction 1 with reaction 2 or 3 affords the catalytic reaction 4,  $(R_F)_3P + XO \rightarrow (R_F)_3PO + X$ ; no reaction occurs in the absence of the Mo catalyst. The kinetics of catalysis were examined by monitoring the concentrations of reactants and products by <sup>19</sup>F NMR spectroscopy. After 15 h, each system showed ca. 100 turnovers. Reaction 4 with  $XO = (R_F)_2SO$  has a catalytic rate constant of  $7 \times 10^{-3} M^{-1} s^{-1}$ , close to the value for reaction 1. This and other considerations show that the catalytic rate is limited by the rate of oxo transfer from the Mo(VI) complex  $MoO_2(L-NS_2)$ . An attempt to establish the catalytic mechanism led to detection of inhibition; the inhibitory species could not be identified. These results provide the most detailed information on the kinetics and mechanisms of Mo-mediated oxygen atom transfer and demonstrate the efficacy of <sup>19</sup>F NMR for detecting and monitoring catalysis and determining catalytic velocities and rate constants. The relation of these results to the enzymatic reduction of *N*-oxides and *S*-oxides is briefly discussed.

In this laboratory we have developed analogue reaction systems<sup>2-5</sup> for molybdoenzymes that catalyze the addition or removal of an oxygen atom from generalized substrate X/XO. These enzymes are usually referred to as hydroxylases; their properties have been reviewed in some detail.<sup>6-10</sup> Our working hypothesis

is that at least some of these enzymes catalyze substrate oxidation or reduction by the forward or reverse reaction 1, in which an



oxygen atom is directly transferred to or removed from substrate without obligatory intervention of any other reactant. In this case, we denote the enzymes as oxo-transferases. A system that has proven to be extremely useful is that of reaction 2, which effects stoichiometric reduction of a number of substrates, including *S*-oxides, *N*-oxides, and nitrate, and also stoichiometric oxidation of tertiary phosphines.

The design of analogue reaction systems, with particular attention to requisite properties of the complexes that serve as representations of the Mo-containing catalytic sites, has been considered elsewhere.<sup>3,11,12</sup> Briefly, complexes  $MoO_2(L-NS_2)$  and  $MoO(L-NS_2)(DMF)$  contain coordination units not inconsistent

(1) (a) National Institutes of Health Postdoctoral Fellow, 1985-1987. (b) Overseas Associate, 1986-1988, Department of Biotechnology, Government of India; on leave from the Department of Chemistry, Osmania University, Hyderabad 500007, India.

(2) Berg, J. M.; Holm, R. H. *J. Am. Chem. Soc.* 1984, 106, 3035.

(3) Berg, J. M.; Holm, R. H. *J. Am. Chem. Soc.* 1985, 107, 925.

(4) Harlan, E. W.; Berg, J. M.; Holm, R. H. *J. Am. Chem. Soc.* 1986, 108, 6992.

(5) Caradonna, J. P.; Harlan, E. W.; Holm, R. H. *J. Am. Chem. Soc.* 1986, 108, 7856.

(6) Bray, R. C. In *The Enzymes*; Boyer, P. D., Ed.; Academic: New York, 1975; Vol. XII, Part B, Chapter 6.

(7) Bray, R. C. *Adv. Enzymol. Relat. Areas Mol. Biol.* 1980, 51, 107.

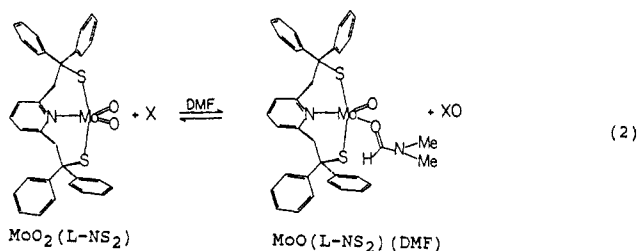
(8) Coughlan, M. P., Ed. *Molybdenum and Molybdenum-Containing Enzymes*; Pergamon: New York, 1980.

(9) Spiro, T. G., Ed. *Molybdenum Enzymes*; Wiley-Interscience: New York, 1985.

(10) Holm, R. H. *Chem. Rev.* 1987, 87, 1401.

(11) Holm, R. H.; Berg, J. M. *Pure Appl. Chem.* 1984, 56, 1645.

(12) Holm, R. H.; Berg, J. M. *Acc. Chem. Res.* 1986, 19, 363.



with Mo EXAFS results for several enzymes<sup>13</sup> and are sufficiently sterically encumbered so as to suppress reaction leading to formation of an oxo-bridged Mo(V) dimer. An important aspect of the coordination unit is the presence of thiolate sulfur atoms, which have the property of setting the effective Mo(VI) reduction potential at a point where MoO<sub>2</sub>(L-NS<sub>2</sub>) is reducible to MoO(L-NS<sub>2</sub>)(DMF) by (at least) Ph<sub>3</sub>P<sup>3</sup> and arenethiols.<sup>4,5</sup> As seen from the structure of MoO<sub>2</sub>(L-NS<sub>2</sub>),<sup>14</sup> one phenyl ring of each *gem*-diphenyl group overlies a Mo=O bond, thereby providing an apparent barrier to the formation of an oxo bridge. There is no evidence for the existence of other than mononuclear catalytic sites in oxo-transferases.

At this stage of development of oxo-transferase structural and reactivity analogues, the system represented by reaction 2 is the most realistic biologically. While not an overly demanding but nonetheless obligatory criterion in this context,<sup>4,12</sup> MoO(L-NS<sub>2</sub>)(DMF) does reduce actual enzymatic substrates, including nicotinamide *N*-oxide,<sup>4</sup> *d*-biotin *S*-oxide,<sup>3</sup> and nitrate.<sup>15</sup> Rate constants for the reduction of substrates have been determined only for *S*-oxides and only at ambient temperature.<sup>3</sup> In order to provide a more detailed analysis of the kinetics and mechanism of oxo transfer in reaction 2, the temperature dependencies of rate constants and associated activation parameters for the oxidation of a tertiary phosphine and the reduction of an *S*-oxide and a pyridine *N*-oxide have been determined. Oxidation and reduction reactions have been coupled to produce systems in which the oxidized substrates are catalytically reduced, and the course of catalysis has been investigated by an NMR method. These results are reported in full here and are considered in relation to reactions catalyzed by oxo-transferases.

### Experimental Section

**Preparation of Compounds.** MoO<sub>2</sub>(L-NS<sub>2</sub>) and MoO(L-NS<sub>2</sub>)(DMF),<sup>14</sup> bis(*p*-fluorophenyl) sulfide and sulfoxide,<sup>16</sup> tris(*p*-fluorophenyl)phosphine and phosphine oxide,<sup>17</sup> and 3-fluoropyridine *N*-oxide<sup>18</sup> were prepared by published methods. 3-Fluoropyridine was obtained from Aldrich.

**Reactions and Kinetics.** All reactions were carried out under strictly anaerobic conditions in solutions of DMF (Burdick and Jackson), which was stored over 4-Å molecular sieves and degassed prior to use. Substrate oxidation and reductions were monitored spectrophotometrically with a Cary 219 spectrophotometer equipped with a thermostated cell compartment. Kinetics analyses follow the methods developed earlier.<sup>3</sup> In the system MoO<sub>2</sub>(L-NS<sub>2</sub>) + (*p*-FC<sub>6</sub>H<sub>4</sub>)<sub>3</sub>P, [Mo(VI)]<sub>0</sub> = 2.0–2.3 mM and [phosphine]<sub>0</sub> was 2.5–3.0 times higher. At each temperature at least three runs with different reactant mole ratios were conducted, and reactions were followed through at least 3 half-lives. Values of the second-order rate constants *k*<sub>2</sub> were obtained by minimizing the function of eq 3, where the absorbance values were taken at 530 (*i* = 1) and 450 (*i*

$$Q = \sum_{i=1}^2 \sum_j [A_{ij}^{\text{obsd}}(t_j) - A_{ij}^{\text{calcd}}(t_j)]^2 \quad (3)$$

= 2) nm. The calculated absorbance at time *t*<sub>*j*</sub>, *A*<sub>*ij*</sub><sup>calcd</sup>(*t*<sub>*j*</sub>), is given by *A*<sub>*ij*</sub><sup>calcd</sup>(*t*<sub>*j*</sub>) = *b*{ $\epsilon_1$ [MoO<sub>2</sub>(L-NS<sub>2</sub>)] +  $\epsilon_2$ [MoO(L-NS<sub>2</sub>)(DMF)]}, in which *b* is the path length and the extinction coefficients<sup>14</sup> are  $\epsilon_1$  = 600,  $\epsilon_2$  =

**Table I.** Rate Constants for the Reaction of MoO<sub>2</sub>(L-NS<sub>2</sub>) with (R<sub>F</sub>)<sub>3</sub>P at Different Temperatures

<i>T</i> , K	<i>k</i> <sub>2</sub> × 10 <sup>3</sup> , M <sup>-1</sup> s <sup>-1</sup>
287.5	5.0 ± 0.2
297.5	9.7 ± 0.4
307.5	22.0 ± 1.0
317.5	41.5 ± 1.9

3900,  $\epsilon_2^1$  = 6280, and  $\epsilon_2^2$  = 2170 M<sup>-1</sup> cm<sup>-1</sup>. Estimates of the uncertainty in *k*<sub>2</sub> were given by the standard deviations obtained from repeated minimizations of function 3 (500 cycles) in which each independent *A*<sub>*ij*</sub><sup>obsd</sup>(*t*<sub>*j*</sub>) point was randomly varied within its accuracy limit (±3.3%). The expression for the time dependence of the concentrations of the Mo(VI) and Mo(IV) complexes has been given earlier.<sup>3</sup>

In the systems MoO(L-NS<sub>2</sub>)(DMF) + XO = 3-FC<sub>6</sub>H<sub>4</sub>NO and (*p*-FC<sub>6</sub>H<sub>4</sub>)<sub>2</sub>SO, [Mo(IV)]<sub>0</sub> = 0.40–0.45 mM and [XO]<sub>0</sub> was 8–160 times higher, corresponding to pseudo-first-order conditions. At each temperature, a minimum of five runs with different reactant mole ratios were carried out. In obtaining rate constants *k*<sub>1</sub>, we minimized the function of eq 4, in which *i* denotes different [XO] values and  $\sigma(V^{\text{obsd}})$  is the

$$\chi^2 = \sum_i [V_i^{\text{obsd}} - V_i^{\text{calcd}}]^2 / \sigma(V_i^{\text{obsd}})^2 \quad (4)$$

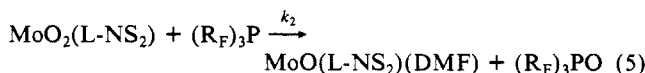
standard deviation in the observed reaction velocity *V*<sup>obsd</sup> (±4.6%) determined from linear regression analysis. Each ln(*A*<sub>*i*</sub> - *A*<sub>∞</sub>) value was randomly varied within its error limit (±3.5%). The uncertainties in *k*<sub>2</sub> and equilibrium constant *K*<sub>eq</sub> were estimated by standard deviations calculated from multiple least-squares minimizations of function 4 (500 cycles) in which each *V*<sup>obsd</sup> point was randomly varied within its error bounds.

**Catalysis.** Catalytic systems consisted of (*p*-FC<sub>6</sub>H<sub>4</sub>)<sub>3</sub>P, substrate ((*p*-FC<sub>6</sub>H<sub>4</sub>)<sub>2</sub>SO or 3-FC<sub>6</sub>H<sub>4</sub>NO), and MoO<sub>2</sub>(L-NS<sub>2</sub>) as catalyst. Reactions were followed by <sup>19</sup>F NMR spectroscopy with use of a Bruker WM spectrometer operating at 284 MHz; chemical shifts are referenced to CFC<sub>3</sub> external standard. Usually for each system, [Mo(VI)]<sub>0</sub> = 5–10 mM, [(*p*-FC<sub>6</sub>H<sub>4</sub>)<sub>2</sub>SO]<sub>0</sub> = [3-FC<sub>6</sub>H<sub>4</sub>NO]<sub>0</sub> = 1000 mM, and [(*p*-FC<sub>6</sub>H<sub>4</sub>)<sub>3</sub>P]<sub>0</sub> was varied between 30 and 1000 mM. The following <sup>19</sup>F *T*<sub>1</sub> values were determined by the inversion-recovery method with proton broad-band decoupling in DMF-*d*<sub>7</sub> solutions at 30 °C and 1.5 M in fluorine atoms: (*p*-FC<sub>6</sub>H<sub>4</sub>)<sub>3</sub>P, 3.8 s; (*p*-FC<sub>6</sub>H<sub>4</sub>)<sub>3</sub>PO, 3.5 s; 3-FC<sub>6</sub>H<sub>4</sub>N, 11.9 s; 3-FC<sub>6</sub>H<sub>4</sub>NO, 7.4 s; (*p*-FC<sub>6</sub>H<sub>4</sub>)<sub>2</sub>S, 9.9 s; (*p*-FC<sub>6</sub>H<sub>4</sub>)<sub>2</sub>SO, 5.8 s. Suitable NMR acquisition parameters were employed to avoid saturation and afford reliable integrated intensities. Spectra were treated with a trapezoidal window function and zero-filled to 16K prior to Fourier transformation and integration. Uncertainties in catalytic velocities (vide infra) were estimated by standard deviations calculated from multiple least-squares minimization (500 cycles) in which each intensity point, ln{[(R<sub>F</sub>)<sub>3</sub>P] + [(R<sub>F</sub>)<sub>3</sub>PO]} / [(R<sub>F</sub>)<sub>3</sub>P], was randomly varied within its error limits. No appreciable decomposition of MoO<sub>2</sub>(L-NS<sub>2</sub>) was detected in the systems studied.

### Results

The kinetics of oxidation of (*p*-FC<sub>6</sub>H<sub>4</sub>)<sub>3</sub>P by MoO<sub>2</sub>(L-NS<sub>2</sub>) and reduction of (*p*-FC<sub>6</sub>H<sub>4</sub>)<sub>2</sub>SO and 3-fluoropyridine *N*-oxide by MoO(L-NS<sub>2</sub>)(DMF) in DMF solutions at 287.5–317.5 K have been determined. Hereafter, R<sub>F</sub> = *p*-C<sub>6</sub>H<sub>4</sub>F and the *N*-oxide is designated as 3-FpyO. Individual reactions are first investigated, followed by a description of catalytic oxygen atom (oxo) transfer systems based on these reactions. Fluorinated substrates were utilized to permit monitoring of the catalytic systems by <sup>19</sup>F NMR spectroscopy. The utility of this procedure has already been demonstrated in the catalytic reduction of (R<sub>F</sub>)<sub>2</sub>SO by R<sub>F</sub>SH.<sup>5</sup>

**Phosphine Oxidation.** Absorption maxima of MoO<sub>2</sub>(L-NS<sub>2</sub>) at 385 and 449 nm decrease, while the features of MoO(L-NS<sub>2</sub>)(DMF) at 365, 528, and 734 nm increase, in intensity as reaction 5 proceeds. Tight isosbestic points occur at 386 and 473



$$d[\text{MoO}_2(\text{L-NS}_2)]/dt = -k_2[\text{MoO}_2(\text{L-NS}_2)][(\text{R}_F)_3\text{P}] \quad (6)$$

nm. The time course of spectral change (not shown) is completely analogous to that of the oxidation of Ph<sub>3</sub>P, which is depicted elsewhere.<sup>3</sup> The final spectrum shows quantitative formation of the Mo(IV) complex. The reaction follows the second-order rate law 6; its integrated form has been given elsewhere.<sup>3</sup> Analysis

(13) (a) Cramer, S. P.; Wahl, R.; Rajagopalan, K. V. *J. Am. Chem. Soc.* **1981**, *103*, 7721. (b) Cramer, S. P.; Solomonson, L. P.; Adams, M. W. W.; Mortenson, L. E. *J. Am. Chem. Soc.* **1984**, *106*, 1467. (c) Cramer, S. P.; Hille, R. *J. Am. Chem. Soc.* **1985**, *107*, 8164. (d) Cramer, S. P. *Adv. Inorg. Bioinorg. Mech.* **1983**, *2*, 259.

(14) Berg, J. M.; Holm, R. H. *J. Am. Chem. Soc.* **1985**, *107*, 917.

(15) Craig, J. A.; Holm, R. H., results to be published.

(16) (a) Leonard, N. J.; Sutton, L. E. *J. Am. Chem. Soc.* **1948**, *70*, 1564.

(b) Wilson, G. E., Jr.; Chang, M. M. Y. *J. Am. Chem. Soc.* **1974**, *96*, 7533.

(17) Johnson, A. W.; Jones, H. L. *J. Am. Chem. Soc.* **1968**, *90*, 5232.

(18) Bellas, M.; Suschitzky, H. *J. Chem. Soc.* **1963**, 4007.

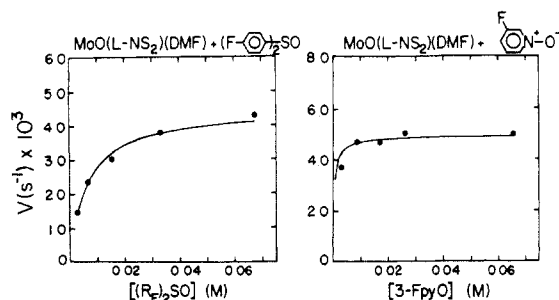


Figure 1. Dependence of the velocity of reaction 7 with XO = (R<sub>F</sub>)<sub>2</sub>SO and 3-FpyO on the substrate concentration, demonstrating saturation kinetics at sufficiently high [XO].

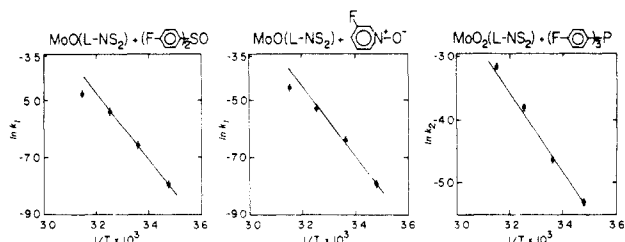


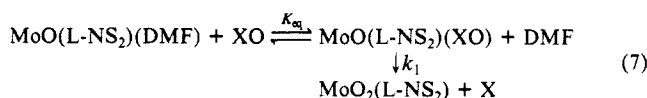
Figure 2. Eyring plots of the rate constants of reactions 7 (XO = (R<sub>F</sub>)<sub>2</sub>SO and 3-FpyO) and 5.

Table II. Rate Constants for the Reactions of MoO(L-NS<sub>2</sub>)(DMF) with S-Oxide and N-Oxide Substrates at Different Temperatures

T, K	k <sub>1</sub> × 10 <sup>4</sup> , s <sup>-1</sup>	
	(R <sub>F</sub> ) <sub>2</sub> SO	3-FpyO
287.5	3.5 ± 0.2	3.7 ± 0.2
297.5	14.0 ± 0.7	16.0 ± 0.8
307.5	45.0 ± 2.3	49.0 ± 2.5
317.5	84.0 ± 4.2	102.0 ± 5.1

of the absorbance data leads to the rate constants in Table I. The value  $k_2(297.5 \text{ K}) = 9.7(4) \times 10^{-3} \text{ M}^{-1} \text{ s}^{-1}$  is close to  $k_2(296 \text{ K}) = 7(1) \times 10^{-3} \text{ M}^{-1} \text{ s}^{-1}$  for the oxidation of Ph<sub>3</sub>P by MoO<sub>2</sub>(L-NS<sub>2</sub>).<sup>3</sup>

**Substrate Reduction.** MoO(L-NS<sub>2</sub>)(DMF) is quantitatively oxidized by excess XO = (R<sub>F</sub>)<sub>2</sub>SO or 3-FpyO in the same two-step process 7 that applies to the reduction of other sulfoxides.<sup>3</sup> As



the reaction progresses, clean isobestic points are developed at 386 and 473 nm. The final spectrum is identical with that of MoO<sub>2</sub>(L-NS<sub>2</sub>). The reaction is first order in the Mo(IV) complex, as shown by linear plots of ln(A<sub>t</sub> - A<sub>∞</sub>) vs time in systems containing greater in 8 equiv of (R<sub>F</sub>)<sub>2</sub>SO or 3-FpyO. Reaction rates were evaluated from slopes of these plots. Typical plots of the rate dependence on substrate concentration for both substrates are shown in Figure 1. At adequately high values of [XO], substrate saturation kinetics prevail.

In scheme 7, reaction is initiated in the form of reversible substrate binding followed by intramolecular oxo transfer with rate constant k<sub>1</sub>. The scheme is described by rate law 8 (Y = DMF + XO) and the reaction velocity is given by eq 9. Fits of

$$d[\text{MoO(L-NS}_2\text{)Y}]/dt = -k_1[\text{MoO(L-NS}_2\text{)(XO)}] = -k_1\{K_{\text{eq}}[\text{XO}]/(K_{\text{eq}}[\text{XO}] + [\text{DMF}])\}[\text{MoO(L-NS}_2\text{)Y}] \quad (8)$$

$$V = k_1\{K_{\text{eq}}[\text{XO}]/(K_{\text{eq}}[\text{XO}] + [\text{DMF}])\} \quad (9)$$

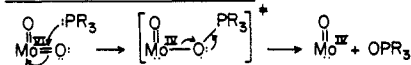
the observed rate data to eq 9 yielded values of k<sub>1</sub> and K<sub>eq</sub>. Rate constants are collected in Table II. The data also fit the inverse of eq 9, affording the corresponding linear double-reciprocal plots (not shown). The rate constant  $k_1(297.5 \text{ K}) = 1.40(7) \times 10^{-3} \text{ s}^{-1}$  is indistinguishable from  $1.43(3) \times 10^{-3} \text{ s}^{-1}$  for the reduction

Table III. Activation Parameters for Oxo-Transfer Reactions

reaction <sup>a</sup>	ΔH <sup>‡</sup> , kcal/mol	ΔS <sup>‡</sup> , cal/(deg mol)	ref
Substrate Oxidation			
MoO <sub>2</sub> (L-NS <sub>2</sub> ) + (R <sub>F</sub> ) <sub>3</sub> P	11.7 ± 0.6	-28.4 ± 1.6	b
MoO <sub>2</sub> (ssp)(DMF) + Et <sub>2</sub> PhP	15.6	-20.7	19
MoO <sub>2</sub> (sse)(DMF) + Et <sub>2</sub> PhP	16.8	-19.7	19
MoO <sub>2</sub> (L-Cys OEt) <sub>2</sub> + Ph <sub>3</sub> P	11	-37	20
[RuO(bpy) <sub>2</sub> (py)] <sup>2+</sup> + Me <sub>2</sub> S	8.0 ± 0.9	-26 ± 3	21
[RuO(bpy) <sub>2</sub> (py)] <sup>2+</sup> + Me <sub>2</sub> SO	6.8 ± 0.2	-39 ± 3	21
Substrate Reduction			
MoO(L-NS <sub>2</sub> )(DMF) + 3-FpyO	23.4 ± 1.4	7.2 ± 2.0	b
MoO(L-NS <sub>2</sub> )(DMF) + (R <sub>F</sub> ) <sub>2</sub> SO	22.1 ± 1.3	2.6 ± 1.6	b

<sup>a</sup>ssp = (2-salicylideneamino)benzenethiolate(2-); sse = 2-(salicylideneamino)ethanethiolate(2-). <sup>b</sup>This work.

• Oxo Transfer to Substrate



• Oxo Transfer from Substrate

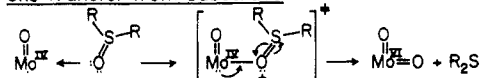


Figure 3. Proposed transition states for reactions 5 and 7; the latter is illustrated with use of an S-oxide.

of Ph<sub>2</sub>SO at 296 K; other sulfoxides are reduced by MoO(L-NS<sub>2</sub>)(DMF) with nearly the same rate constants.<sup>3</sup> For the reduction of 3-FpyO,  $k_1(297.5 \text{ K}) = 1.60(8) \times 10^{-3} \text{ s}^{-1}$ , essentially identical with that for sulfoxide reduction.

**Mechanisms.** Activation parameters for the preceding three reactions were obtained from the least-squares fits of rate constants to the Eyring equation 10, shown in Figure 2. Values are listed

$$\ln k_{1,2} = (k_B T/h) \exp[\Delta S^{\ddagger}/R - \Delta H^{\ddagger}/RT] \quad (10)$$

in Table III<sup>19-21</sup> together with the very limited additional data for oxo transfer. In this work, estimated errors were determined by measuring the effect on the linear regression results of randomly varying each rate constant within its uncertainty range.

Activation entropies are consistent with reaction order. The value ΔS<sup>‡</sup> = -28.4 (1.6) eu for bimolecular reaction 5 requires an associative transition state. As for related systems,<sup>3,10,22</sup> a feasible reaction pathway involves attack of the nucleophilic phosphine on the vacant π\* orbitals of a Mo<sup>VI</sup>=O group followed by development of a transition state with Mo<sup>IV</sup> character and reduction of the Mo-O bond order of the reacting group to near one in the course of forming a P-O bond. This transition state is depicted in Figure 3.

The small activation entropies for reduction of (R<sub>F</sub>)<sub>2</sub>SO and 3-FpyO in reaction 7 strongly suggest that the structure of the ground-state precursor complex, MoO(L-NS<sub>2</sub>)(XO), in the first-order path and that of the activated complex have the similarities evident from the depiction of the latter in Figure 3. The most important feature would be retention of a Mo-OX bonding interaction. Elsewhere, we have argued that the small variation of binding constants and rate constants for sulfoxide reduction with major structural changes around the sulfur atom provides strong evidence for Mo-O bonding of substrate.<sup>3</sup> It appears unlikely that Mo<sup>VI</sup> character is fully developed in the transition states inasmuch as this would imply formation of the Mo<sup>VI</sup>O<sub>2</sub> group and a concomitant diminished affinity to retain the substrate, now in the reduced form, as part of the activated complex. Note that the activation entropy for reduction of the S-oxide, in

(19) Topich, J.; Lyon, J. T., III. *Inorg. Chem.* **1984**, *23*, 3202.

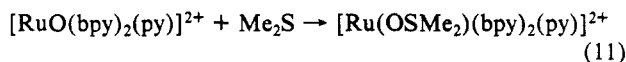
(20) Deli, J.; Speier, G. *Transition Met. Chem.* **1981**, *6*, 227.

(21) Roecker, L.; Dobson, J. C.; Vining, W. J.; Meyer, T. J. *Inorg. Chem.* **1987**, *26*, 779.

(22) Reynolds, M. S.; Berg, J. M.; Holm, R. H. *Inorg. Chem.* **1984**, *23*, 3057.

particular, is virtually zero (2.6 (1.6) eu).

The other oxo-transfer reaction systems in Table III have activation parameters comparable to those for reactions 5 and 7. Of particular pertinence to the question of mechanism is the oxidation of dimethyl sulfide by Ru<sup>IV</sup>O in reaction 11.<sup>21</sup> The



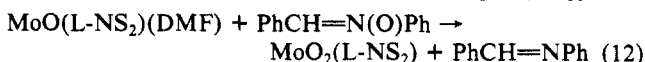
reaction is first order in each reactant with a rate constant of 17.1 (3) M<sup>-1</sup> s<sup>-1</sup> in acetonitrile solution at 25 °C, and the activation parameters are  $\Delta H^\ddagger = 8.0$  (9) kcal/mol and  $\Delta S^\ddagger = -26$  (3) eu. Here the immediate product of oxo transfer, the O-bound Ru(II) sulfoxide complex, could be identified from its absorption spectrum. Because in the following step this intermediate isomerizes to the S-bound form, it is even more probable that the transition state is O-bonded. This provides a reasonable precedent for the transition state for substrate oxidation depicted in Figure 3. The activation entropy for reaction 11 is closely comparable to that for reaction 5, implying but certainly not requiring similar transition states in the two cases.

**Thermodynamics of N-Oxide Reduction.** We have devised a thermodynamic reaction scale for oxo-transfer reactions, which is described at some length elsewhere.<sup>4,10</sup> The scale consists of reactions of the type  $\text{X} + \frac{1}{2}\text{O}_2(\text{g}) = \text{XO}$  with an associated enthalpy change  $\Delta H$  usually obtained from thermodynamic compilations. When arranged in the order of decreasing  $\Delta H$ , the scale may be used in the manner of a table of standard potentials. The reduced member of a given reaction is thermodynamically competent to reduce the oxidized member of any other reaction with a larger  $\Delta H$ , and conversely. The stoichiometric reduction of 3-FpyO and other heterocyclic N-oxides<sup>4</sup> by MoO(L-NS<sub>2</sub>)-(DMF) shows that the oxidation enthalpies of these substrates are larger than ca. -35 kcal/mol, the established upper limit for the MoO(L-NS<sub>2</sub>)(DMF) +  $\frac{1}{2}\text{O}_2 \rightarrow \text{MoO}_2(\text{L-NS}_2)$  oxidation reaction.<sup>4</sup> However, it has not been possible to place heterocyclic amine/N-oxide reactions accurately in the thermodynamic scale of oxo donor propensities.

Recently, Kirchner et al.<sup>23</sup> provided the first determination of the dissociation enthalpies of



bonds from the combustion enthalpies of imino and diazene N-oxides. The values cover the range 63.3 (7)–79.2 (9) kcal/mol. When combined with the dissociation enthalpy of dioxygen (59.55 (2) kcal/mol), oxidation enthalpies on our scale range from -3.8 (PhCH=N(O)Ph) to -19.7 (C<sub>3</sub>H<sub>7</sub>N=N(O)C<sub>3</sub>H<sub>7</sub>) kcal/mol. In accordance with these results, reaction 12 with [Mo(IV)]<sub>0</sub> = 0.9



mM and excess substrate proceeded to completion (in about 2 h). (The reaction of PhN=N(O)Ph (-17.4 kcal/mol) resulted in decomposition of the Mo(IV) complex.) The tridentate Schiff base complexes MoO(sap)(DMF) and MoO(ssp)(DMF)<sup>24</sup> also reduced the N-oxide to the imine, which was identified in all cases by TLC. On the thermodynamic reaction scale, PhCH=N(O)Ph is a more powerful oxo donor than Me<sub>2</sub>SO by 23 kcal/mol and a less powerful donor than *t*-BuOOH by about 19 kcal/mol. When the entire scale is considered,<sup>10</sup> this N-oxide is a moderately strong oxo donor. There are no determinations of N–O bond enthalpies of pyridine or other heterocyclic N-oxides, but it is very likely that their values will fall in or close to the above range. However, the reduction of PhN=N(O)Ph is much slower than that of pyO or 3-FpyO.

**Catalytic Oxo Transfer.** The occurrence of reactions 5 and 7, involving oxygen atom transfer to and from substrate, suggests

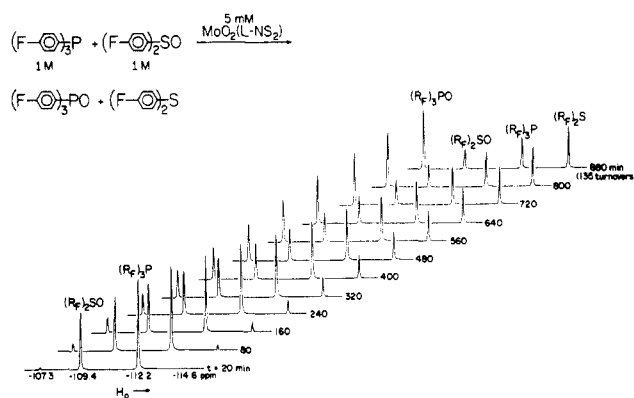


**Figure 4.** Time course (to 880 min and 135 turnovers) of the Mo-catalyzed oxo-transfer reaction between (R<sub>F</sub>)<sub>3</sub>P and (R<sub>F</sub>)<sub>2</sub>SO in DMF solution at 30 °C as observed by <sup>19</sup>F NMR spectroscopy. In this and the following figure, initial concentrations, signal assignments, and chemical shifts vs CFCl<sub>3</sub> external standard are indicated.

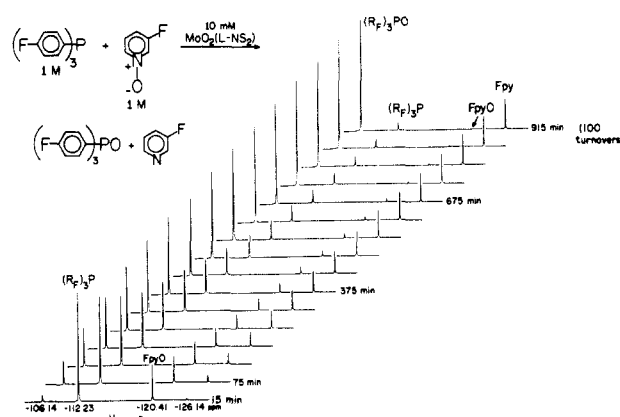
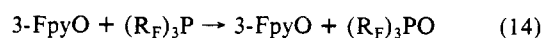
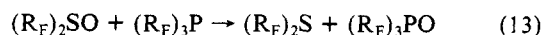


**Figure 5.** Time course (to 915 min and 100 turnovers) of the Mo-catalyzed oxo-transfer reaction between (R<sub>F</sub>)<sub>3</sub>P and 3-FpyO as observed by <sup>19</sup>F spectroscopy under the conditions of Figure 4.

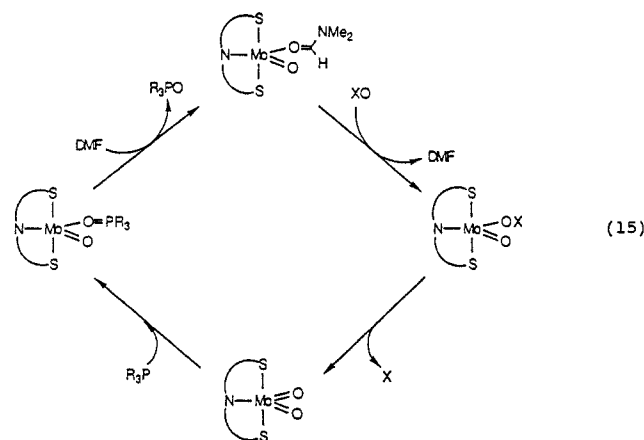
that the two processes could be coupled in the form of catalytic reactions 13 and 14. Demonstration of catalysis is provided in



Figures 4 and 5. The reactions are very effectively monitored by <sup>19</sup>F spectroscopy because of the base-line resolution of the four signals in each system. Concentrations at various times were determined by signal integration. In Figure 4, representing reaction 13, (R<sub>F</sub>)<sub>2</sub>SO (-109.4 ppm) and (R<sub>F</sub>)<sub>3</sub>P (-112.2 ppm) are consumed while (R<sub>F</sub>)<sub>3</sub>PO (-107.3 ppm) and (R<sub>F</sub>)<sub>2</sub>S (-114.6 ppm) are produced in precisely equal amounts. In Figure 5, depicting reaction 14, the situation is completely analogous: 3-FpyO (-120.4 ppm) and (R<sub>F</sub>)<sub>3</sub>P (-126.1 ppm) are consumed and 3-FpyO (-126.1 ppm) and (R<sub>F</sub>)<sub>3</sub>PO are generated in equimolar amounts. Both systems were very well behaved. Chemical shifts of products agreed with those of authentic samples, the total sum of integrated intensities was constant, systems remained homogeneous over the entire course of monitoring, and no additional <sup>19</sup>F resonances were observed in the -70 to -140 ppm range. In the examples shown, reaction 13 was followed through 880 min or 135 turnovers, and reaction 14 for 915 min or about 100 turnovers. This example of reaction 14 was allowed to proceed to completion. In the absence of the Mo complex, neither system in DMF solution showed any detectable reaction (from <sup>19</sup>F spectra) for at least 120 h at 25 °C. These results demonstrate the operation of catalytic cycle 15 (XO = N-oxide, S-oxide). We have previously demonstrated this cycle for Me<sub>2</sub>SO as a substrate,<sup>3</sup> but the concentrations of substrate and product could not be readily followed with time.

(23) Kirchner, J. J.; Acree, W. E., Jr.; Pilcher, G.; Shaofeng, L. *J. Chem. Thermodyn.* **1986**, *18*, 793.

(24) Boyd, I. W.; Spence, J. T. *Inorg. Chem.* **1982**, *21*, 1602. In this paper the abbreviations sip = sap and sma = ssp are used. The molecularity of the Mo<sup>IV</sup>O complexes prepared in this reference has not been established.



The kinetics of the component half-reactions of the two systems indicate that phosphine oxidation is expected to be rate-limiting. The second-order rate constant for reaction 5 at 297.5 °C is  $k_2 = 9.7(4) \times 10^{-3} \text{ M}^{-1} \text{ s}^{-1}$ . This rate constant should be compared with the pseudo-second-order rate constant for substrate reduction by reaction 7,  $k_1 K_{\text{eq}} / [\text{DMF}] \approx 1 \text{ M}^{-1} \text{ s}^{-1}$  at 297.5 °C for both substrates since their first-order rate constants  $k_1$  are nearly identical. The lack of any significant change in the Mo chromophore during catalytic turnover is consistent with this value being 2 orders of magnitude larger than  $k_2$ . Thus, reaction 7 is relatively rapid, leading to a fairly constant  $[\text{MoO}(\text{L-NS}_2)(\text{DMF})]$  throughout catalysis. Inasmuch as this complex is degraded by excess phosphine, the success of the catalytic system depends on an adequately fast rate of oxidation of this complex by *S*-oxide or *N*-oxide.

Under the preceding conditions, the disappearance of  $(\text{R}_F)_3\text{P}$  is governed by the first-order decay relationship 16, where  $k_c$  is

$$[(\text{R}_F)_3\text{P}] = [(\text{R}_F)_3\text{P}]_0 \exp(k_c [\text{MoO}_2(\text{L-NS}_2)] t) \quad (16)$$

the rate constant of catalysis. With the constraint on total phosphine concentration  $[(\text{R}_F)_3\text{P}]_0 = [(\text{R}_F)_3\text{P}] + [(\text{R}_F)_3\text{PO}]$ , eq 16 can be restated as eq 17. A similar relationship holds for the

$$\ln \left( \frac{[(\text{R}_F)_3\text{P}] + [(\text{R}_F)_3\text{PO}]}{[(\text{R}_F)_3\text{P}]} \right) = k_c [\text{MoO}_2(\text{L-NS}_2)] t \quad (17)$$

substrates XO/X. For the two catalytic systems, the relative concentrations of reactants and products were determined at 20 min intervals over ca. 15 h from the integrated intensities of  $^{19}\text{F}$  resonances. Plots of  $\ln \{[(\text{R}_F)_3\text{P}] + [(\text{R}_F)_3\text{PO}]\} / [(\text{R}_F)_3\text{P}]$  vs  $t$  were linear over the entire period. This is another indication of catalyst stability, which in the present systems is improved over that containing  $\text{Ph}_3\text{P}$  and  $\text{Me}_2\text{SO}$ .<sup>3</sup> Typical behavior is exhibited by the system in Figure 6, where  $[(\text{R}_F)_3\text{P}]_0 = 100 \text{ mM}$ ,  $[(\text{R}_F)_2\text{SO}]_0 = 700 \text{ mM}$ , and  $[\text{MoO}_2(\text{L-NS}_2)] = 5.0 \text{ mM}$ . The slope gives the catalytic velocity  $v = 3.6 \times 10^{-3} \text{ s}^{-1}$ . Further,  $v / [\text{Mo}(\text{VI})] = k_c = 7.2 \times 10^{-3} \text{ M}^{-1} \text{ s}^{-1}$ , close to rate constant  $k_2$  of reaction 5. This result shows that the catalytic rate is limited by the rate of oxo transfer from  $\text{MoO}_2(\text{L-NS}_2)$ , as would be additionally expected from the approximate ratio  $1.0/0.0097 \approx 100$  for the second-order rate constants for oxo transfer from *S*-oxide and to phosphine in reaction 13. The same result holds for reaction system 14.

Having defined the kinetics of catalysis, we directed our attention to the investigation of mechanism such that it could be classified into one of the two major categories,<sup>25</sup> sequential or ping-pong. Chicken liver sulfite oxidase, for example, operates by a ping-pong mechanism.<sup>26</sup> An attempt to classify the catalytic cycle by determining initial velocity patterns is shown in Figure 7. This plot was obtained by varying  $[(\text{R}_F)_3\text{P}]$  at constant molybdenum concentration; catalytic velocities were determined from

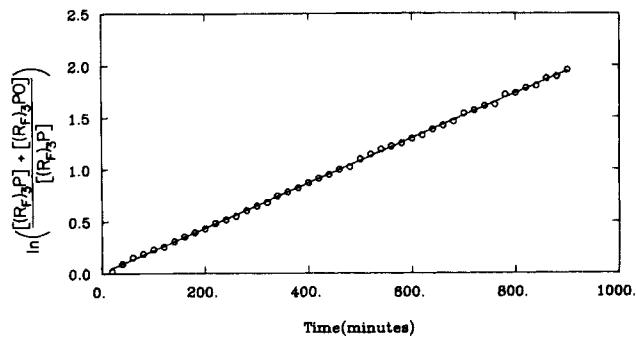


**Figure 6.** Plot of  $\ln \{[(\text{R}_F)_3\text{P}] + [(\text{R}_F)_3\text{PO}]\} / [(\text{R}_F)_3\text{P}]$  vs time at 30 °C for a system initially containing 5.0 mM  $\text{MoO}_2(\text{L-NS}_2)$ , 100 mM  $(\text{R}_F)_3\text{P}$ , and 700 mM  $(\text{R}_F)_2\text{SO}$  in DMF. The solid line is a least-squares fit to the points. This plot is typical for systems whose concentrations were varied within the limits given in the Experimental Section.

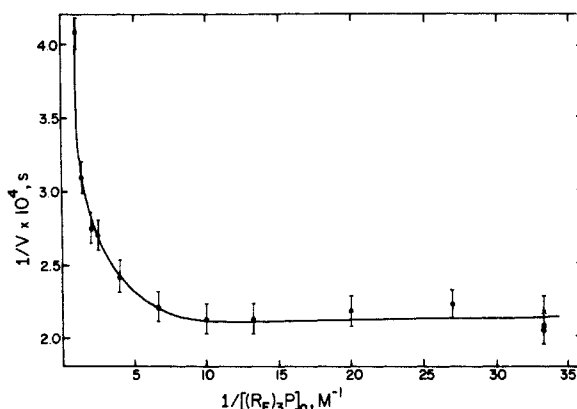


**Figure 7.** Plot of the reciprocal catalytic specific velocities ( $1/k_c$ ) and phosphine concentrations in DMF solutions of systems with  $[(\text{R}_F)_2\text{SO}]_0 = 1000$  (●), 700 (■), 100 (×) mM,  $[(\text{R}_F)_3\text{P}] = 30\text{--}1000 \text{ mM}$ , and  $[\text{MoO}_2(\text{L-NS}_2)] = 4.5\text{--}5.1 \text{ mM}$ . The curve is intended only as a rough locus of points.

plots of the phosphine concentration function vs time. Nearly all points correspond to  $[(\text{R}_F)_2\text{SO}] = 1000 \text{ mM}$ . It is immediately evident that this curve does not resemble the linear behavior expected for an uncomplicated sequential or ping-pong pathway. Further, in the concentration regime where linear behavior appears to be approached ( $1/[(\text{R}_F)_3\text{P}] \gtrsim 10$ ), velocities proved to be rather insensitive to variations of *S*-oxide concentrations down to 100 mM. The latter is a practical limit in these systems for accurate monitoring of concentrations by the  $^{19}\text{F}$  NMR method.

In the sequential mechanism, all reactants and catalyst combine prior to any reaction taking place or any product released. This mechanism appears to be a priori improbable based on the X-ray structure of  $\text{MoO}_2(\text{L-NS}_2)$ , which we have argued to be resistant to six-coordination because of ligand conformation and steric hindrance offered by the *gem*-diphenyl groups.<sup>14</sup>  $\text{MoO}(\text{L-NS}_2)(\text{DMF})$  possesses a replaceable solvate ligand, which allows binding of substrate or product, but binding of both appears unlikely. These observations argue against an associative mechanism of this sort. Of course, the many instances of the occurrence of the forward and reverse reaction 2<sup>3,4</sup> make it obvious that only substrate and molybdenum complex are required to effect oxo transfer to or from substrate.

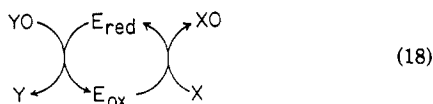
The trace in Figure 7 for the catalytic system of reaction 13 is reminiscent of substrate inhibition in a ping-pong system. In the normal ping-pong mechanism, product is released from the catalyst before all substrates are added. At high  $[(\text{R}_F)_3\text{P}]$  the velocity is less than at intermediate concentrations. At relatively low  $[(\text{R}_F)_3\text{P}]$ , the *S*-oxide can compete more effectively for a binding site of  $\text{MoO}(\text{L-NS}_2)(\text{DMF})$ , but the velocity decreases owing to a decrease in the rate-determining phosphine oxidation step. We suspect that the phosphine inhibits by binding to  $\text{Mo}(\text{IV})$ , but we have not been able to demonstrate independently the formation of a  $\text{MoO}(\text{L-NS}_2)(\text{DMF})/(\text{R}_F)_3\text{P}$  adduct or any

(25) (a) Cleland, W. W. In *Investigations of Rates and Mechanisms of Reactions*, 4th ed., Part I; Bernasconi, C. F., Ed.; Vol. VI in *Techniques of Chemistry*; Wiley-Interscience: New York, 1986; Chapter XII. (b) Cleland, W. W. *Adv. Enzymol.* **1977**, *45*, 273.

(26) Kessler, D. L.; Rajagopalan, K. V. *J. Biol. Chem.* **1972**, *247*, 6566.

other species that might inhibit catalysis. These components do react, resulting in a bleaching of the Mo(IV) chromophore, but we have been unsuccessful in determining the nature of the initial reaction product. Any additional, meaningful analysis of the catalytic system requires specification of the inhibitory step(s). This matter notwithstanding, the present investigation does provide a clear demonstration of the utility of  $^{19}\text{F}$  NMR spectroscopy in detecting and monitoring catalysis and determining catalytic velocities and rate constants.

Lastly, we have noted elsewhere<sup>4</sup> the current evidence for the operation of oxo transfer in reconstituted enzyme systems by means of the generalized cycle 18. Both aldehyde oxidase<sup>27-31</sup> and



xanthine oxidase<sup>32-34</sup> can utilize certain *N*-oxides or *S*-oxides YO in the presence of substrates X to yield products XO under anaerobic conditions. In several cases, X has been replaced by a reducing agent, mercaptoethanol, such that YO can be considered the substrate. Thus these enzymes are, in addition to their usual functions, *N*-oxide and *S*-oxide reductases. An important experiment in the present context is that by Murray et al.,<sup>33</sup> who showed partial transfer of  $^{18}\text{O}$  from labeled nicotinamide *N*-oxide to product uric acid by xanthine oxidase, thereby proving at least

one step of direct enzymatic oxo transfer. The analogy between cycles 15 and 18 is apparent, particularly in view of the demonstration that benzenethiol can be used as a reductant of Mo(VI).<sup>5</sup> Recently, Friedman et al.<sup>35</sup> demonstrated  $^{15}\text{N}$  and  $^{18}\text{O}$  labeling in nitrite/nitrate enzymatic interconversion. These results require oxo transfer to and from the catalytic site, but it has not yet been shown that the enzyme in question is molybdenum dependent.

The definitive results to date on direct atom transfer by molybdoenzymes follow from the single-turnover experiments of Hille and Sprecher.<sup>36</sup> When  $^{18}\text{O}$ -labeled milk xanthine oxidase was incubated with a stoichiometric deficiency of xanthine in ordinary water, the oxygen atom incorporated into uric acid is at least 79% enriched in the isotope label. In the reverse experiment, using  $^{18}\text{O}$ -labeled  $\text{H}_2\text{O}$  and unlabeled enzyme, the uric acid product contained 90%  $^{16}\text{O}$  at the position of reaction. While this enzyme is perhaps better denoted as a hydroxylase than an oxo-transferase in view of a probable hydrolytic reaction<sup>36,37</sup> at the molybdenum site liberating uric acid, the reaction pathway unambiguously involves oxygen atom transfer. Xanthine oxidase, as well as aldehyde oxidase, contains the Mo<sup>VI</sup>OS group in its oxidized form.<sup>13a,d,38-40</sup> Development of functional model systems for these enzymes first requires stabilization of this group in a suitable complex. Experiments pertinent to this matter are in progress.

**Acknowledgment.** This research was supported by National Science Foundation Grant CHE 85-21365. We thank Dr. J. M. Berg and E. W. Harlan for useful discussions and E.W.H. for experimental assistance.

- (27) Shimokawa, O.; Ishimoto, M. *J. Biochem.* **1979**, *86*, 1709.  
 (28) Tatsumi, K.; Kitamura, S.; Yamada, H. *Chem. Pharm. Bull.* **1982**, *30*, 4585; *Biochim. Biophys. Acta* **1983**, *747*, 86.  
 (29) Kitamura, S.; Tatsumi, K. *Biochem. Biophys. Res. Commun.* **1984**, *120*, 602.  
 (30) Yoshihara, S.; Tatsumi, K. *Arch. Biochem. Biophys.* **1985**, *242*, 213.  
 (31) Yoshihara, S.; Tatsumi, K. *Arch. Biochem. Biophys.* **1986**, *249*, 8.  
 (32) Murray, K. N.; Chaykin, S. *J. Biol. Chem.* **1966**, *241*, 2029, 3468.  
 (33) Murray, K. N.; Watson, G.; Chaykin, S. *J. Biol. Chem.* **1966**, *241*, 4798.  
 (34) Stöhrer, G.; Brown, G. B. *J. Biol. Chem.* **1969**, *244*, 2498.

- (35) Friedman, S. H.; Masefski, W., Jr.; Hollocher, T. C. *J. Biol. Chem.* **1986**, *261*, 10538.  
 (36) Hille, R.; Sprecher, H. *J. Biol. Chem.* **1987**, *262*, 10914.  
 (37) Bray, R. C.; George, G. N. *Biochem. Soc. Trans.* **1985**, *13*, 560.  
 (38) Barber, M. J.; Coughlan, M. P.; Rajagopalan, K. V.; Siegel, L. M. *Biochemistry* **1982**, *21*, 3561.  
 (39) Bray, R. C.; George, G. N.; Gutteridge, S.; Norlander, L.; Stell, J. G. P.; Stubbley, C. *Biochem. J.* **1982**, *203*, 263.  
 (40) Hille, R.; Massey, V. In ref 9, Chapter 9.